PHYSICAL REVIEW D **73,** 084013 (2006)

Black rings, boosted strings, and Gregory-Laflamme instability

Jordan L. Hovdebo[1,2,*] and Robert C. Myers[1,2,†]

[1]*Perimeter Institute for Theoretical Physics, 31 Caroline Street North, Waterloo, Ontario N2L 2Y5, Canada*
[2]*Department of Physics, University of Waterloo, Waterloo, Ontario N2L 3G1, Canada*

(Received 24 January 2006; published 14 April 2006)

We investigate the Gregory-Laflamme instability for black strings carrying KK momentum along the internal direction. We demonstrate a simple kinematical relation between the thresholds of the classical instability for the boosted and static black strings. We also find that Sorkin's critical dimension depends on the internal velocity and in fact disappears for sufficiently large boosts. Our analysis implies the existence of an analogous instability for the five-dimensional black ring of Emparan and Reall. We also use our results for boosted black strings to construct a simple model of the black ring and argue that such rings exist in any number of space-time dimensions.

DOI: 10.1103/PhysRevD.73.084013 PACS numbers: 04.50.+h, 04.70.Bw

I. INTRODUCTION

After many years of investigation, higher-dimensional general relativity still continues to be a rich source of new ideas and physics. It is now 80 years ago that Kaluza [1] and Klein [2] first entertained the idea of general relativity in higher dimensions as a route towards the unification of gravity with the other forces in nature. Their nascent explorations laid foundations for modern superstring and M theory. The study of higher-dimensional general relativity provides important insights into the structure of these theories. Further, in recent braneworld scenarios, the extra dimensions are much larger than the Planck scale and so the study of classical Einstein equations in higher dimensions is necessary to understand the phenomenology of these models.

While there has been a great deal of activity studying ''black objects'' in higher dimensions, particularly in string theory [3], there is clear evidence that our four-dimensional intuition leads us astray in thinking about the physics of event horizons in higher-dimensional gravity. For example, an interesting corollary of the early theoretical investigations of black holes in four dimensions was that each connected component of a stationary horizon must have the topology of a two-sphere [4]. However, this result is easily evaded in higher dimensions. As a simple example, consider the four-dimensional Schwarschild metric combined with a flat metric on R^m. This space-time is an extended black hole solution of Einstein's equations in $4 + m$ dimensions, and the topology of the horizon is $S^2 \times R^m$. Clearly, this straightforward construction is easily extended to constructing many other higher-dimensional black holes whose horizons inherit the topology of the ''appended'' manifold.[1] These solutions describe extended objects in that the geometry is not asymptotically flat in all $3 + m$ spatial directions and so one might have conjectured that all localized black objects would have a spherical horizon. However, this hope was eliminated by Emparan and Reall [6] who constructed an explicit five-dimensional metric describing a black ring with horizon topology $S^2 \times S^1$. The circle direction in these solutions is supported against collapse by angular momentum carried in this direction, as was anticipated much earlier in [7].

These black ring solutions also eliminated any possibility of extending the usual black hole uniqueness theorems beyond four dimensions. In four-dimensional general relativity, work on black hole uniqueness theorems began with the pioneering work of Israel [8]. The no-hair results are now rigorously established for Einstein gravity coupled to Maxwell fields and various other simple matter systems [9]. While in string theory we study more complicated matter field couplings (as well as space-time dimensions beyond four), the plethora of new solutions [3] still respected the spirit of the no-hair theorems in that the black hole geometries are still completely determined by some small set of charges. However, the black rings [6] explicitly provided two solutions for which the mass and spin were degenerate with five-dimensional spinning black holes [7]. This nonuniqueness was further extended to a continuous degeneracy with the introduction of dipole charges [10].

One open question is whether or not such black rings exist in more than five dimensions. One argument suggesting that five dimensions is special comes from considering the scaling of the Newtonian gravitational and centripetal forces. In this sense, five dimensions is unique in that it is only for $D = 5$ that these forces scale in the same way and can be stably balanced. Of course, this is purely a classical argument which need not be true in the fully relativistic theory and, further, it ignores the tension of the ring. It is part of the goal of this paper to address this question.

In considering spinning black holes and rings, four dimensions is also distinguished from higher dimensions by the Kerr bound. While there is an upper bound on the angular momentum per unit mass of a four-dimensional black hole, no such bound exists for black holes in dimen-

*Email address: jlhovdeb@sciborg.uwaterloo.ca
†Email address: rmyers@perimeterinstitute.ca

[1]Similar solutions arise for four dimensions in the presence of a negative cosmological constant [5].

sions higher than five [7]. The five-dimensional black rings also remove this bound in higher dimensions [6].

Even more strikingly, in contrast to the stability theorems proven for four-dimensional black holes [11], Gregory and Laflamme [12,13] have shown that extended black branes are unstable. The spectrum of metric perturbations contains a growing mode that causes a ripple in the apparent horizon. The endpoint of the instability is not completely clear; however, a fascinating picture is emerging [14]. Interestingly, it was shown in [15] that the Gregory-Laflamme instability dynamically enforces the ''Kerr bound'' for $D \geq 6$. Perhaps a stability criterion will restore some of the restrictions which are seen to apply to black holes in four dimensions.

In the present paper, we investigate the Gregory-Laflamme instability for black strings carrying Kaluza-Klein (KK) momentum. These solutions are easily constructed by boosting the static black string metrics. We begin in Sec. II with a review of the Gregory-Laflamme instability for static black strings. The discussion of boosted black strings begins in Sec. III, where we first present the solutions carrying KK momentum and then consider their stability with global thermodynamic arguments. We then adapt the usual numerical analysis of the Gregory-Laflamme instability to these boosted solutions. We demonstrate a simple kinematical relation between the thresholds of the instability for boosted and static black strings with a fixed horizon radius. Comparing the numerical results with the previous global analysis, we find that Sorkin's critical dimension [16] depends on the boost velocity. In Sec. IV, we apply our results to a discussion of the stability of the black ring solutions of Emparan and Reall [6]. As already anticipated there, we find that large black rings will suffer from a Gregory-Laflamme instability. Our analysis allows us to argue that black rings will exist in any dimension higher than five as well.

II. GREGORY-LAFLAMME INSTABILITY

The detailed calculation of the instability of the boosted black strings will be an extension of the original analysis of Gregory and Laflamme [12,13]. Hence we begin here by reviewing the stability analysis for static black strings.[2] For the static string in $D = n + 4$ dimensions, the background metric can be written as

$$ds^2 = -f(r)dt^2 + \frac{dr^2}{f(r)} + r^2 d\Omega_{n+1}^2 + dz^2, \tag{2.1}$$

where $d\Omega_{n+1}^2$ is the metric on a unit $(n+1)$-sphere and

$$f(r) = 1 - \left(\frac{r_+}{r}\right)^n. \tag{2.2}$$

The event horizon is situated at $r = r_+$ and we imagine that the z direction is periodically identified with $z = z + 2\pi R$.

Now we seek to solve the linearized Einstein equations for perturbations around the above background (2.1). The full metric is written as

$$g_{\mu\nu} = \tilde{g}_{\mu\nu} + h_{\mu\nu}, \tag{2.3}$$

where $\tilde{g}_{\mu\nu}$ is the background metric (2.1) and $h_{\mu\nu}$ is the small perturbation. We will restrict the stability analysis to the S-wave sector on the $(n+1)$-sphere as it can be proven that modes with $\ell \neq 0$ are all completely stable. This is apparent following the line of argument originally presented in [18]. Assume the threshold for any instability should correspond to a time-independent mode. This mode can then be analytically continued to a negative mode of the Euclidean Schwarzschild solution; however, Gross, Perry and Yaffe [19] have shown that the existence of such a mode is unique to the S-wave sector. Hence we write the perturbations as

$$h_{\mu\nu} = \mathcal{R}e[e^{\Omega t + ikz} a_{\mu\nu}(r)], \tag{2.4}$$

where Ω and k are assumed to be real and $a_{\mu\nu}$ is chosen to respect the spherical symmetry, e.g., $a_{z\theta} = 0$. Hence solutions with $\Omega > 0$ correspond to instabilities of the static black string. The above ansatz (2.4) can be further simplified with infinitesimal diffeomorphisms. Using a diffeomorphism with the same t and z dependence as above, the perturbation may be reduced to a form where the only nonvanishing components of $a_{\mu\nu}$ are

$$\begin{gathered} a_{tt} = h_t(r), \qquad a_{rr} = h_r(r), \qquad a_{zz} = h_z(r), \\ a_{tr} = \Omega h_v(r), \qquad a_{zr} = -ikh_v(r). \end{gathered} \tag{2.5}$$

Note that even though $a_{\theta\theta} = 0 = a_{\phi\phi}$, these perturbations can cause rippling in the position of the *apparent* horizon along the internal direction [13].

The linearized Einstein equations give a set of coupled equations determining the four radial profiles above. However, we may eliminate h_v, h_r and h_t from these equations to produce a single second order equation for h_z:

$$h_z''(r) + p(r)h_z'(r) + q(r)h_z(r) = \Omega^2 w(r) h_z(r), \tag{2.6}$$

$$\begin{aligned} p(r) &= \frac{1}{r}\left(1 + \frac{n}{f(r)} - \frac{4(2+n)k^2r^2}{2k^2r^2 + n(1+n)(\frac{r_+}{r})^n}\right), \\ q(r) &= \frac{1}{r^2}\left(-\frac{k^2r^2}{f(r)}\,\frac{2k^2r^2 - n(3+n)(\frac{r_+}{r})^n}{2k^2r^2 + n(1+n)(\frac{r_+}{r})^n}\right), \\ w(r) &= \frac{1}{f(r)^2}. \end{aligned} \tag{2.7}$$

[2]Note, however, that our gauge fixing follows [17] which differs from that in the original analysis of [12,13]. The present gauge fixing [17] has the advantages that it succeeds in completely fixing the gauge and it is well behaved in the limit of vanishing k.

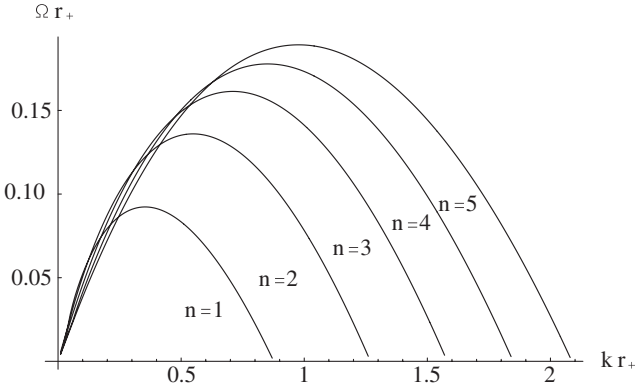

FIG. 1. Unstable frequencies and wave numbers for the static black string.

Next we must determine the appropriate boundary conditions on $h_z(r)$ at the horizon and asymptotic infinity for a physical solution. First, near the horizon, the radial equation (2.6) simplifies considerably yielding solutions

$$h_z = Ae^{\Omega r_*} + Be^{-\Omega r_*}. \tag{2.8}$$

Here r_* is the tortoise coordinate defined by $dr_*/dr = 1/f$ and with which the horizon appears at $r_* \to -\infty$. Now, in principle, we would choose initial data for the perturbation on a Cauchy surface extending to the future horizon and demand that the perturbation be finite there. Hence we require that $B = 0$ for physical solutions.[3]

Equation (2.6) also simplifies as $r \to \infty$. The asymptotic solutions behave differently depending on whether $n = 1$ or $n \geq 2$. For $n = 1$, the regular solutions take the form

$$h_z \sim e^{-\mu r} r^{2-[(\Omega^2+\mu^2)/2\mu]r_+}, \tag{2.9}$$

where $\mu^2 \equiv \Omega^2 + k^2$. For $n \geq 2$, they are

$$h_z \sim e^{-\mu r} r^{(n+3)/2}, \tag{2.10}$$

with the same definition for μ. Hence we expect that the unstable perturbations are localized near the horizon with a characteristic size μ^{-1}.

The instabilities can be determined as follows: For a fixed value of k, we choose Ω and set the asymptotic conditions according to Eq. (2.9) or (2.10). The radial equation (2.6) is integrated in numerically to $r \approx r_+$. Here we match the numerical solution to the near-horizon solution (2.8) which determines the ratio B/A for the chosen value of Ω. By varying Ω, we may tune this ratio to satisfy the physical boundary condition at the horizon, i.e., $B = 0$. We find solutions for a range of k from 0 up to a maximum value $k_{\max}$. Figure 1 shows the resulting solutions for various space-time dimensions. The critical value $k_{\max}$ corresponds to the threshold of the Gregory-Laflamme instability and is set by the only dimensionful parameter in the background, r_+, up to a factor of order one. Table I tabulates $k_{\max}$ for different values of n.

[3]While the present argument is somewhat superficial, a more careful treatment yields the same result [12,13].

TABLE I. Maximum wave number corresponding to the marginally unstable mode of the static black string in various dimensions $D = n + 4$.

n	1	2	3	4	5
$k_{\max} r_+$	0.876	1.269	1.581	1.849	2.087

When the coordinate along the string is periodic, the allowed values of k are discrete, i.e., for $z = z + 2\pi R$, $k = n/R$ with n an integer. Hence for small R, the system is stable when $k_{\max} \geq 1/R$. However, for $R > 1/k_{\max}$, the lowest wave number, allowed by periodicity, falls in the unstable range and the black string is unstable.

III. BOOSTED BLACK STRINGS

Our focus at present is "boosted black strings," i.e., stationary black string solutions carrying momentum along their length. Such solutions can be obtained by simply boosting the static solution (2.1) along the z direction,

$$ds^2 = -dt^2 + \frac{dr^2}{f(r)} + r^2 d\Omega_{n+1}^2 + dz^2 + (1-f)\cosh^2\beta(dt + \tanh\beta dz)^2, \tag{3.1}$$

where the boost velocity is given by $v = \tanh\beta$, and as before

$$f(r) = 1 - \left(\frac{r_+}{r}\right)^n. \tag{3.2}$$

Again, we assume that in the new solution the z direction is periodically identified with $z = z + 2\pi R$. This solution has an event horizon situated at r_+ and an ergosurface at $r = r_+\cosh^{2/n}\beta$, where ∂_t becomes spacelike.

To see quantitatively that this solution carries both mass and momentum, we calculate the Arnowitt, Deser, and Misner (ADM)-like stress tensor for the string with the following asymptotic integrals [20]:

$$T_{ab} = \frac{1}{16\pi} G \oint d\Omega_{n+1} \hat{r}^{n+1} n^i \times [\eta_{ab}(\partial_i h^c{}_c + \partial_i h^j{}_j - \partial_j h^j{}_i) - \partial_i h_{ab}]. \tag{3.3}$$

Here n^i is a radial unit vector in the transverse subspace and $h_{\mu\nu} = g_{\mu\nu} - \eta_{\mu\nu}$ is the deviation of the asymptotic metric from flat space. Note that the index labels $a, b, c \in \{t, z\}$, while i, j run over the transverse directions. To apply this formula, the asymptotic metric must approach that of flat space in Cartesian coordinates. This is accomplished with the coordinate transformation $r = \hat{r}(1 + (r_+/\hat{r})^n/2n)$ which yields

$$ds^2 \simeq -\left(1-\left(\frac{r_+}{\hat{r}}\right)^n \cosh^2\beta\right)dt^2 + 2\left(\frac{r_+}{\hat{r}}\right)^n \sinh\beta\cosh\beta dt dz + \left(1+\left(\frac{r_+}{\hat{r}}\right)^n \sinh^2\beta\right)dz^2 + \left(1+\frac{1}{n}\left(\frac{r_+}{\hat{r}}\right)^n\right)dx^i dx_i, \tag{3.4}$$

keeping only the leading order corrections. Here $\hat{r}^2 = \sum_{i=1}^{n+2}(x^i)^2$. Hence applying Eq. (3.3), we find that the stress energy for the boosted black string is

$$T_{tt} = \frac{\Omega_{n+1}}{16\pi G} r_+^n (n\cosh^2\beta + 1),$$
$$T_{tz} = \frac{\Omega_{n+1}}{16\pi G} r_+^n n\cosh\beta\sinh\beta, \tag{3.5}$$
$$T_{zz} = \frac{\Omega_{n+1}}{16\pi G} r_+^n (n\sinh^2\beta - 1),$$

where Ω_{n+1} is the area of a unit $(n+1)$-sphere. Integrating over z, the total energy and momentum of the string are then

$$E_{\rm BS} = \frac{\Omega_{n+1}R}{8G} r_+^n (n\cosh^2\beta + 1), \tag{3.6}$$

$$P_{\rm BS} = \frac{\Omega_{n+1}R}{8G} r_+^n n\cosh\beta\sinh\beta. \tag{3.7}$$

The limit of maximal boost $\beta \to \infty$ results in divergent $E_{\rm BS}$, $P_{\rm BS}$, but these can be kept finite if r_+ vanishes sufficiently fast. In particular, taking the large β limit while holding $r_+^n \cosh^2\beta$ fixed produces finite charges. However, the limiting background has a naked null singularity at the center of a finite-size ergosphere.

A. Comparing black strings and black holes

Gregory and Laflamme [12,13] originally gave a simple argument favoring instability of the static black string by comparing its entropy to that of a spherical black hole with the same energy. This argument also plays a role in deducing the full phase structure of black strings and black holes in a compactified space-time [14,21]. So we begin here by extending this discussion of the global thermodynamic stability to the boosted black string. The analysis for the case at hand becomes slightly more complicated because, as well as matching the energy, we must also explicitly match the KK momentum along the z circle in our comparison.

We compare the boosted black string solution (3.1) to a D-dimensional spherical black hole of radius r'_+ moving along the z axis with velocity $v' = \tanh\beta'$. At rest, the energy of the spherical black hole is [7]

$$M_{\rm BH} = \frac{(n+2)\Omega_{n+2}}{16\pi G} r_+'^{\,n+1}.$$

Now, to a distant observer, the spherical black hole behaves like a point particle and so, when boosted, its energy and momentum are given by

$$E_{\rm BH} = M_{\rm BH}\cosh\beta', \qquad P_{\rm BH} = M_{\rm BH}\sinh\beta'. \tag{3.8}$$

Equating the above to those for the black string given in Eqs. (3.6) and (3.7), the black hole must have

$$\tanh\beta' = \frac{n\cosh\beta\sinh\beta}{1+n\cosh^2\beta},$$
$$r_+'^{\,n+1} = 2\pi r_+^n R \frac{\sqrt{1+n(n+2)\cosh^2\beta}}{n+2}\frac{\Omega_{n+1}}{\Omega_{n+2}}. \tag{3.9}$$

It is interesting to note that, with the usual relation $v = \tanh\beta$, the first expression above can be rewritten as

$$v' = v\frac{n}{n+1-v^2}. \tag{3.10}$$

Hence we always have $v' < v$, with v' approaching v (from below) as $v \to 1$.

We now need to calculate the horizon entropy $S = A/4G$ for each configuration. For the boosted string, we find

$$S_{\rm BS} = \frac{\pi R\Omega_{n+1}}{2G} r_+^{n+1}\cosh\beta. \tag{3.11}$$

The $\cosh\beta$ dependence arises here because proper length along the z direction at the horizon expands with increasing β, as can be seen from Eq. (3.1). In contrast, the horizon area of the black hole is invariant under boosting. This invariance is easily verified in the present case by explicitly applying a boost along the z direction to the black hole metric in isotropic coordinates. However, this is a general result [22]. Hence for the boosted black hole, we have

$$S_{\rm BH} = \frac{\Omega_{n+2}}{4G} r_+'^{\,n+2}. \tag{3.12}$$

Setting $S_{\rm BH}/S_{\rm BS} = 1$ and solving for R, we find

$$R_{\rm min} = \frac{r_+}{2\pi\cosh\beta}\frac{(n+2)^{n+2}}{(n(n+2)+\cosh^{-2}\beta)^{n/2+1}}\frac{\Omega_{n+2}}{\Omega_{n+1}}. \tag{3.13}$$

Hence we might expect that the boosted black string is unstable for $R > R_{\rm min}$. Fixing r_+, $R_{\rm min}$ scales like $1/\cosh\beta$ for large β. It should be remembered that the large β limit with r_+ fixed has divergent energy. Rescaling r_+ while taking the large β limit can make the energy finite, but this causes $R_{\rm min}$ to vanish even more quickly. In any event, this naive analysis suggests that the instability will persist for $\beta \to \infty$. Again, note that the black string horizon becomes a null singularity in this limit.

B. Instability of boosted strings

Turning now to the instability of boosted strings, a natural choice of coordinates in which to perform the

analysis are those for which the string appears at rest:

$$\tilde{t} = \cosh\beta t + \sinh\beta z, \qquad \tilde{z} = \cosh\beta z + \sinh\beta t. \tag{3.14}$$

In the following we shall refer to this as the "static frame," and our original frame (3.1), having simple periodic boundary conditions in z, will be called the "physical frame."

Let us begin in the static frame with perturbations having functional form $\exp(\tilde{\Omega}\,\tilde{t} + i\tilde{k}\,\tilde{z})$. Now transforming back to the physical frame, this becomes $\exp(\Omega t + ikz)$ where

$$\Omega = \cosh\beta\tilde{\Omega} + i\sinh\beta\tilde{k}, \qquad k = \cosh\beta\tilde{k} - i\sinh\beta\tilde{\Omega}. \tag{3.15}$$

For real $\tilde{k}$ and $\tilde{\Omega}$, the imaginary part of k induced by the boost is inconsistent with the periodic boundary conditions on z, which are imposed in the physical frame. Hence consistency requires that we add an imaginary part to $\tilde{k}$, $i\tanh\beta\tilde{\Omega}$, which ensures that the resulting k is real. In practice, finding solutions also requires adding a small imaginary part to $\tilde{\Omega}$—see below. Hence, in the static frame, our perturbations have a $\tilde{t}$, $\tilde{z}$ dependence of the form

$$\exp[(\tilde{\Omega} + i\tilde{\omega})\tilde{t} + i(\tilde{k} + i\tanh\beta\tilde{\Omega})\tilde{z}], \tag{3.16}$$

where $\tilde{\Omega}$, $\tilde{\omega}$, $\tilde{k}$ are all real. In the physical frame, the t, z dependence then becomes $\exp(\Omega t)\exp i(\omega t + kz)$ where

$$\Omega = \tilde{\Omega}/\cosh\beta, \qquad \omega = \cosh\beta\tilde{\omega} + \sinh\beta,\tilde{k} \qquad k = \cosh\beta\tilde{k} + \sinh\beta\tilde{\omega}. \tag{3.17}$$

Again, all of the above are real numbers. Provided we ensure that k is a multiple of $1/R$, this ansatz is now consistent with the periodicity of z. As before, solutions with $\Omega > 0$ will correspond to instabilities.

Including the complex part, $i\tilde{\omega}$, in the near-horizon form of the solution (2.8) turns the terms, respectively, into ingoing and outgoing modes at the future-event horizon. When $\tilde{\Omega} > 0$, regularity of the solution requires that we set $B = 0$, as before. For the special case that $\tilde{\Omega}$ vanishes, neither solution diverges on the future-event horizon; however, the limit of the second is undefined there. In this case, we continue to impose $B = 0$ as our boundary condition for $\tilde{\Omega} = 0$, as this corresponds to a boundary condition of purely ingoing modes at the future-event horizon.

Hence the problem of finding instabilities of the boosted string reduces to finding instabilities of the static string with the complex frequencies defined by (3.16). With these frequencies, the perturbations have a time-dependent phase. A boundary condition must therefore be imposed on both the real and imaginary parts of the unknown function. This means that for each value of $\tilde{k}$ there are two constraints that must be solved on the horizon, precisely matching the number of free parameters $\tilde{\omega}$, $\tilde{\Omega}$. Apart from these complications, the solutions were found numerically using the method outlined in Sec. II.

The numerical results for the frequencies $\tilde{\Omega}$ and $\tilde{\omega}$ in the static frame are displayed as a function of $\tilde{k}$ in Fig. 2 for $n = 1$. The results in other dimensions are similar. On the left, we see that $\tilde{\Omega}(\tilde{k})$ is almost independent of the boost velocity v. This result might be interpreted as arising because even when $v = 0$, $\tilde{\Omega}$ is suppressed relative to $\tilde{k}$ and so making v nonzero (but small) only yields a small perturbation on the unboosted results. Further, we note that the behavior of $\tilde{\Omega}(\tilde{k})$ near $\tilde{k} = 0$ and $\tilde{k}_{\max}$ is essentially independent of v—a point we return to below.

More dramatic differences are seen when the results are transformed to the physical frame with Eq. (3.17). We display $\Omega(k)$ in Fig. 3(a) for $n = 1$. Again, the behavior for other values of n is similar. We might note that the comparison is made here for boosted strings with a fixed value of r_+. Hence the total energy (3.6) increases as the boost velocity grows and diverges with $\beta \to \infty$.

In fact, one can predict the threshold for the Gregory-Laflamme instability of the boosted string without the numerical analysis above. The revised ansatz (3.16) in the static frame was introduced to accommodate the time dependence of these modes upon boosting to the physical frame. However, the threshold mode is defined as that where the time dependence (in the static frame) vanishes, i.e., $\tilde{\Omega} = 0$. Hence there is no obstruction to boosting the threshold mode originally found by Gregory and Laflamme. Therefore there is a simple kinematical relation between the thresholds for the boosted and static black

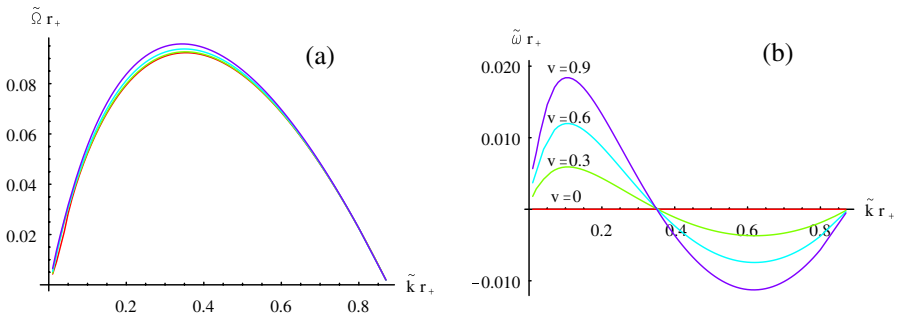

FIG. 2 (color online). Frequencies $\tilde{\Omega}(\tilde{k})$ and $\tilde{\omega}(\tilde{k})$ leading to instabilities, as observed in the static $(\tilde{t}, \tilde{z})$ frame, for $n = 1$.

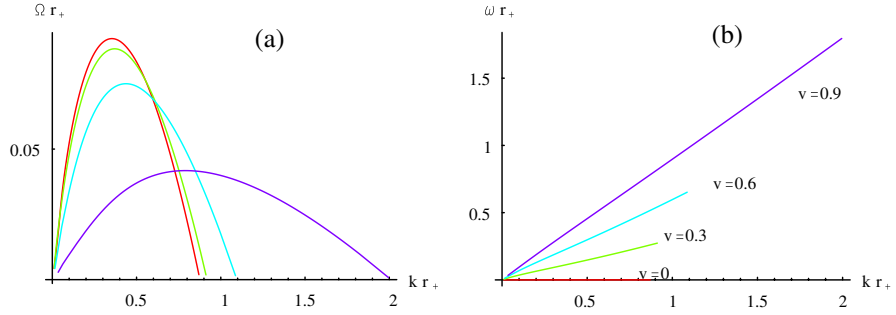

FIG. 3 (color online). Plot of physical frequencies $\Omega(k)$ and $\omega(k)$ leading to boosted string instabilities for fixed horizon size, at various boost velocities and with $n = 1$.

strings. In the physical frame, this marginal mode has

$$k_{\max} = \cosh\beta\tilde{k}_{\max}, \qquad \omega = \sinh\beta\tilde{k}_{\max} \tag{3.18}$$

where $\tilde{k}_{\max}$ is the threshold for a static black string, listed in Table I. Hence these threshold modes are traveling waves in the z direction having precisely the same speed as the boosted string.

One may ask whether there are more general modes with $\tilde{\Omega} = 0$, but nonzero $\tilde{\omega}$. For example, an exactly marginal mode in the physical frame would require that $\tilde{\Omega} = 0$ and $\tilde{\omega} = -\tanh\beta\tilde{k}$, but in fact such a solution is inconsistent with the equations of motion. The linearity of (2.7) allows us to arbitrarily choose a normalization in which h_z is real at a point. When we set $\tilde{\Omega} = 0$, the real and imaginary parts of h_z decouple, implying that h_z is real everywhere. If $\tilde{\omega}$ is nonzero, the only choice of A and B in the near-horizon solution (2.8) consistent with h_z real is $A = B^*$, so that the boundary condition $B = 0$ is not possible. We then conclude that the only solution with $\tilde{\Omega} = 0$ is time independent in the static frame ($\tilde{\omega} = 0$), which is then a traveling wave of constant amplitude in the physical frame.

To close this section, we observe that, in the static frame, $\tilde{\omega}(\tilde{k})$ shows some interesting structure, as shown in Fig. 2(b). The zeros of $\tilde{\omega}$ seem to be independent of v. The vanishing at $\tilde{k}_{\max}$ (and $\tilde{k} = 0$) is understood from the discussion above, but there is also a fixed intermediate zero which seems to coincide with the maximum value of $\tilde{\Omega}$. We do not have a physical explanation for the latter.

Using Eq. (3.17), the phase velocity of the unstable modes in the physical frame can be written as

$$\frac{\omega}{k} = \frac{v + \tilde{\omega}/\tilde{k}}{1 + v\tilde{\omega}/\tilde{k}} \simeq v + (1 - v^2)\frac{\tilde{\omega}}{\tilde{k}} + \cdots. \tag{3.19}$$

The last approximation uses our numerical result that generically $\tilde{\omega}/\tilde{k} \ll 1$. Hence we see that to a good approximation all of the perturbations travel along the string with the boost velocity—a result which is verified by the numerical results in Fig. 3(b). However, given $\tilde{\omega}(\tilde{k})$ in Fig. 2(b), we see that the deviations from this rule are such that the long (short) wavelength modes travel with a phase velocity that is slightly faster (slower) than v. Of course, the threshold mode moves along the z direction with precisely the boost velocity.

C. Comparing black strings and black holes, again

The threshold mode sets a minimum radius for the compact circle for which the boosted black string is unstable. Hence, from Eq. (3.18) above, we have

$$\left(\frac{R_{\min}}{r_+}\right)_{\rm BS} = \frac{1}{(k_{\max}r_+)_{\rm BS}} = \frac{1}{\cosh\beta\tilde{k}_{\max}r_+} \tag{3.20}$$

where again $\tilde{k}_{\max}$ is the static string threshold, given in Table I. This result might be compared to that in Sec. III A. Recall that there we compared the entropy of the boosted black string to that of a small black hole boosted along the z direction. In this case, we found

$$\left(\frac{R_{\min}}{r_+}\right)_{\rm BH} = \frac{1}{(k_{\max}r_+)_{\rm BH}} = \frac{1}{2\pi\cosh\beta}\frac{(n+2)^{n+2}}{(n(n+2) + \cosh^{-2}\beta)^{n/2+1}}\frac{\Omega_{n+2}}{\Omega_{n+1}}. \tag{3.21}$$

Hence the simple scaling with $1/\cosh\beta$ in Eq. (3.20) is modified here by corrections in powers of $1/\cosh^2\beta$. The two results are plotted together in Fig. 4 for various spacetime dimensions.

Considering the static results (i.e., $v = 0$ or $\cosh\beta = 1$), Fig. 4 shows that $(R_{\min})_{\rm BS} > (R_{\min})_{\rm BH}$ for smaller values of D but $(R_{\min})_{\rm BS} < (R_{\min})_{\rm BH}$ for larger values. Sorkin [16] first observed that this transition occurs at a critical dimension between $D = 13$ and $D = 14$.[4] This result indicates that there is an interesting phase diagram [14,21] for $D \leq 13$, with a regime $(R_{\min})_{\rm BS} > R > (R_{\min})_{\rm BH}$ where the black string is locally stable but the black hole solution is the global minimum. Further, these global considerations

[4]In general, the critical dimension depends on the dimension of the black brane and the details of the compactification geometry [23]. Further, the precise value may also depend on the thermodynamic ensemble considered [24].

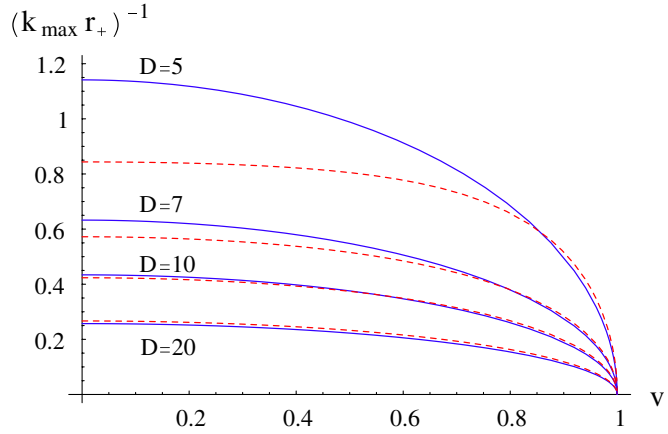

FIG. 4 (color online). Comparison of the threshold wave number calculated numerically (3.20) (blue, solid lines) to that predicted by global entropy considerations (3.21) (red, dashed lines) for $D = 5, 7, 10, 20$.

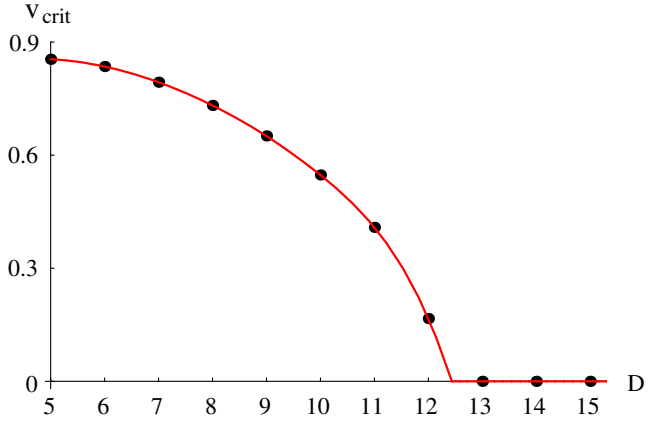

FIG. 5 (color online). The critical boost at which nonuniform black strings become stable in various dimensions. (The curve is simply a guide for the eye.)

then suggest that, in this regime, these two solutions are separated by an unstable solution describing a nonuniform black string [25]—this structure was recently verified with numerical calculations for $D = 6$ [26]. In contrast, for $D > 13$, it appears that the nonuniform black string becomes stable but only appears as the end state of the decay of the uniform black string in the regime $(R_{\rm min})_{\rm BH} > R > (R_{\rm min})_{\rm BS}$ [14].

Now we have observed that $(R_{\rm min})_{\rm BS}$ and $(R_{\rm min})_{\rm BH}$ in Eqs. (3.20) and (3.21) do not have the same dependence on the boost velocity. This leads to an interesting effect which we observe in Fig. 4. In the regime $D \leq 13$, we start with $(R_{\rm min})_{\rm BS} > (R_{\rm min})_{\rm BH}$ for small $\cosh\beta$ but there is a transition to $(R_{\rm min})_{\rm BS} < (R_{\rm min})_{\rm BH}$ for large boosts. Figure 5 displays the critical boost velocity (for the uniform black strings) at which this crossover occurs in various dimensions. This behavior can also be verified using the analytic approximation for the static threshold provided in [16], which yields

$$\left(\frac{R_{\rm min}}{r_+}\right)_{\rm BS} = \frac{1}{(k_{\rm max} r_+)_{\rm BS}} \simeq \frac{1}{2\pi\cosh\beta}\left(\frac{16\pi a\gamma^{n+4}}{(n+1)\Omega_{n+1}}\right)^{1/n} \tag{3.22}$$

where $a \simeq 0.47$ and $\gamma \simeq 0.686$ are constants.

We note that the minimal radius (3.21) from the black hole comparison will receive corrections and these may change the final result. The analysis in Sec. III A treats the black hole as being spherical sitting inside a fixed internal circle. For very small black holes this is an acceptable approximation, but as the size increases, the interactions with the ''image'' black holes in the covering space become important and lead to mass-dependent corrections for the entropy of black holes on cylinders [27]. However, as β increases, so too does the proper separation of the black hole and its images (along the z direction) in their static frame, i.e., $\Delta\tilde{z} = 2\pi R\cosh\beta'$ where the boost factors are related as in Eq. (3.9) but for large boosts, $\cosh\beta' \simeq \cosh\beta$. Naively, Eq. (3.9) shows that the size of the black holes grows at a much slower rate as β increases. However, near the boundary where $S_{\rm BH} = S_{\rm BS}$, one finds that r'_+ grows as $\cosh\beta$ for large β, precisely the same rate as $\Delta\tilde{z}$.

However, tentatively our results show that the critical dimension discovered in [16] depends on the boost velocity and in fact disappears for large values of $\cosh\beta$. Of course, incorporating the compactification corrections for the black holes [27] will allow one to produce a more accurate value for the critical boost in various dimensions [28]. Further, following [16], the critical boost can also be assessed using Gubser's perturbative construction [29] of the nonuniform black string [28].

IV. BLACK RINGS

The question of black hole uniqueness in dimensions greater than four was answered decisively by Emparan and Reall with the construction of an explicit counterexample [6]. Their solution is completely regular on and outside a horizon having topology $S^2 \times S^1$, a black ring. For the metric, we consider the form presented in [30]:

$$\begin{aligned} ds^2 = &-\frac{F(x)}{F(y)}\left(dt + R\sqrt{\lambda\nu}(1+y)d\psi\right)^2 \\ &+ \frac{R^2}{(x-y)^2}\left[-F(x)\left(G(y)d\psi^2 + \frac{F(y)}{G(y)}dy^2\right)\right. \\ &\left. + F(y)^2\left(\frac{dx^2}{G(x)} + \frac{G(x)}{F(x)}d\phi^2\right)\right], \end{aligned} \tag{4.1}$$

where

$$F(\xi) = 1 - \lambda\xi \quad \text{and} \quad G(\xi) = (1-\xi^2)(1-\nu\xi). \tag{4.2}$$

Requiring that the geometry be free of conic singularities when F or G vanish determines the periods of the angles ϕ and ψ as well as sets the value of λ to one of two possibilities,

$$\lambda = \begin{cases} \frac{2\nu}{1+\nu^2} & \text{black ring,} \\ 1 & \text{black hole.} \end{cases} \tag{4.3}$$

With the former choice (x, ϕ) parametrize a two-sphere while ψ is a circle. When $\lambda = 1$, ψ joins with x and ϕ to parametrize a three-sphere and the solution is a five-dimensional Myers-Perry black hole [7] spinning in one plane.

The family of black ring solutions is therefore described by two free parameters, ν and R. The first, ν, can be chosen in the range from 0 to 1 and roughly describes the shape of the black ring. For $\nu \to 0$, the ring becomes increasingly thin and large. In the opposite limit, $\nu \to 1$, the ring flattens along the plane of rotation, becoming a naked ring singularity at $\nu = 1$. R can be roughly thought of as the radius of the ring in a manner that will become apparent shortly.

The ADM energy and spin, as well as the horizon area, are found to be

$$M = \frac{3\pi R^2}{4G} \frac{\lambda(1+\lambda)}{1+\nu}, \tag{4.4}$$

$$J = \frac{\pi R^3}{2G} \frac{(\lambda\nu)^{1/2}(1+\lambda)^{5/2}}{(1+\nu)^2}, \tag{4.5}$$

$$A = 8\pi^2 R^3 \frac{\lambda^{1/2}(1+\lambda)(\lambda-\nu)^{3/2}}{(1+\nu)^2(1-\nu)}. \tag{4.6}$$

A more convenient set of variables for visualizing the various phases of these solutions are the reduced spin, j^2, and area, a_h, defined by

$$j^2 = \frac{27\pi}{32G} \frac{J^2}{M^3} = \begin{cases} \frac{(1+\nu)^3}{8\nu} & \text{black ring,} \\ \frac{2\nu}{1+\nu} & \text{black hole,} \end{cases} \tag{4.7}$$

$$a_h = \frac{3}{16}\sqrt{\frac{3}{\pi}} \frac{A}{(GM)^{3/2}} = \begin{cases} 2\sqrt{\nu(1-\nu)} & \text{black ring,} \\ 2\sqrt{2\frac{1-\nu}{1+\nu}} & \text{black hole.} \end{cases} \tag{4.8}$$

We plot the corresponding quantities in Fig. 6. Note that the black holes are described by $a_h = 2\sqrt{2(1-j^2)}$. The black rings lie on two branches, labeled "large" and "small," which meet at the critical point $\nu = 1/2$.

The large branch corresponds to solutions where the radius of the ring grows more quickly than its thickness, locally approaching the geometry of a boosted string. To see this explicitly, we may take $R \to \infty$, $\nu \to 0$ while keeping $R\nu$ fixed. In this limit, we introduce [30]

$$\begin{aligned} &\nu R = r_+ \sinh^2\beta, \qquad \lambda R = r_+ \cosh^2\beta, \\ &r = -R\frac{F(y)}{y}, \qquad \cos\theta = x, \qquad z = R\psi, \end{aligned} \tag{4.9}$$

and obtain precisely the metric of the boosted black string (3.1). The similarity is in fact more than just local; comparing the horizon area of the black ring in this limit we find that it matches the boosted string result (3.11), implying that we should indeed take R as a measure of the radius of the ring.

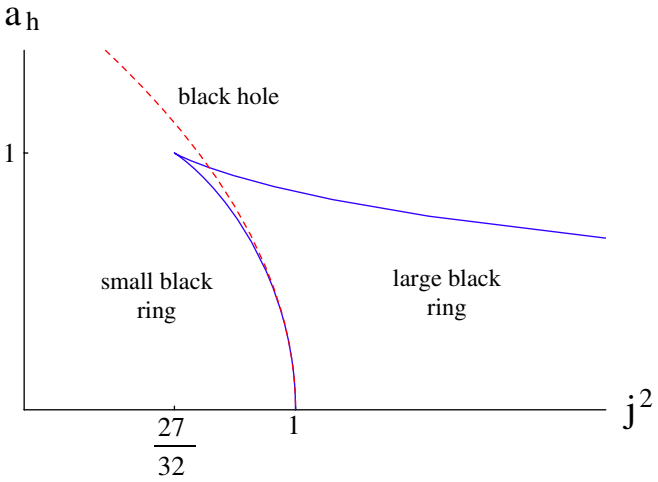

FIG. 6 (color online). Reduced spin and area for the black ring (blue, solid line) and black hole (red, dashed line) solutions described by the metric (4.1). The large (small) ring branch corresponds to $\nu < 1/2$ ($\nu > 1/2$).

Given the similarity between boosted black strings and very large black rings, Emparan and Reall expected that the latter should be subject to a Gregory-Laflamme type instability [6]. Using (3.18), the wave number for the marginal mode of the five-dimensional boosted string is $k_{\max} r_+ \approx 0.876 \cosh\beta$. Translating this result to the black ring variables using (4.9) yields

$$k_{\max} \approx \frac{0.876}{R} \frac{\lambda^{1/2}}{(\lambda-\nu)^{3/2}} \approx \frac{1.239}{R\nu}, \tag{4.10}$$

where the last expression applies only for $\nu \to 0$. Now $k_{\max} \gtrsim 1/R$ should be the condition for the Gregory-Laflamme instability to appear in the black ring.[5] Hence, the above result confirms that the black ring is unstable in the vicinity of small ν. Further, considering the second expression above for arbitrary ν, one finds that $k_{\max} > 1/R$ everywhere which suggests that all of the black rings are unstable. However, we should not think that these calculations are reliable for all values of ν. We consider this question in more detail below by studying a simple model of the black ring.

A. Black strings to black rings

Here we would like to construct a simple model of the black ring that captures its important features. To identify these, we consider the ratio of the mass and spin of the ring from Eqs. (4.4) and (4.5). For small ν, this ratio approaches a constant,

[5]It is important here that the unstable mode is localized near the horizon, which is a point we return to later.

$$\frac{MR}{J} = \frac{3}{\sqrt{2}}[1 - 2\nu + 4\nu^2 + \mathcal{O}(\nu^3)] = \frac{3}{\sqrt{2}}\left[1 - 2\frac{\sqrt{2}GJ}{\pi R^3} + 10\frac{2G^2J^2}{\pi^2R^6} + \mathcal{O}\left(\frac{\sqrt{2}GJ}{\pi R^3}\right)^3\right], \tag{4.11}$$

where implicitly we have expanded the dimensionless quantity $\sqrt{2}GJ/\pi R^3 = \nu + 3\nu^2 + O(\nu^4)$. Our goal is to reproduce this expression with a simple string model. So let us assume we have a spinning loop of string where the loop has a radius R and the string has a linear ''rest mass'' density λ. Then we expect that, up to a boost-dependent factor, the spin is given by $J \sim \lambda R^2$. This allows us to identify the origin of the most important contributions to the energy of the black ring, by reexpressing the contributions in terms of λ and R.

The constant term in Eq. (4.11) corresponds to a contribution to the total energy λR, linear in both factors. Hence, remembering to include the boost dependence, this leading term is simply a combination of the string's rest mass and a kinetic energy. That this term dominates may have been expected since we are considering a limit in which the radius of the ring is large. The next term in the expansion gives a R-independent contribution coming from the gravitational self-energy of the ring in five dimensions, $-G\lambda^2$. The final term in Eq. (4.11) yields a $1/R$ potential which would keep the string from shrinking to zero size when formed in a ring. We can interpret such a contribution as due to rigidity of the string.

Rigidity has appeared before in various string models. In particular, it was argued to be necessary to successfully model the QCD string and was introduced by modifying the Nambu-Goto action by a term dependent on the extrinsic curvature of the world sheet [31]. It was suggested that such a term can emerge when the string is constructed as the compactification of a higher-dimensional brane [32]. Compactifying a three-brane on a two-sphere of radius ρ and forming a loop of string with radius R yields a configuration where the ratio between the tension and rigidity energies is R^2/ρ^2. Comparing this to the ratio of the first and third terms in (4.11) implies that $G\lambda \sim \rho$, whereas for a boosted black string in five dimensions, we have $GT_{tt} \sim r_+$ from Eq. (3.5). This intriguing coincidence suggests that the rigidity of black strings may be accommodated by an extension of the ''membrane paradigm'' [33] to higher dimensions.

Hence we have argued that the gravitational self-interaction and rigidity of the black string play a minor role in determining the configuration for large rings. Now we would like to proceed further in modeling the behavior of such a large black ring by approximating the latter as a loop of black string and using our results for the energy and momentum densities of a boosted black string given in Eq. (3.5). For a loop of string with radius R, these yield a mass and spin

$$M \equiv 2\pi R T_{tt} = xnr_+^n R\left(\cosh 2\beta + 1 + \frac{2}{n}\right), \tag{4.12}$$

$$J \equiv 2\pi R^2 T_{tz} = xnr_+^n R^2 \sinh 2\beta, \tag{4.13}$$

where, for notational convenience, we have introduced the constant $x \equiv \Omega_{n+1}/16G$. Hence we see that our model has three independent parameters: R, r_+ and β, which correspond to the size and thickness of the loop and the tangential boost velocity which determines its angular velocity. Given a configuration with fixed M and J, the above equations give two relations between these parameters but one is left free. Our approach to fixing this last parameter will be demanding that the ring configure itself to maximize its entropy:

$$S = \frac{A}{4G} = 8\pi x r_+^{n+1} R \cosh\beta. \tag{4.14}$$

This is a straightforward although somewhat tedious exercise. Hence we only show the salient steps below.

First, we find it useful to replace R by the dimensionless parameter

$$y \equiv \frac{J}{MR} = \frac{\sinh 2\beta}{\cosh 2\beta + 1 + \frac{2}{n}} \tag{4.15}$$

where the last expression comes from combining Eqs. (4.12) and (4.13). One then determines β and r_+ in terms of y as

$$e^{2\beta} = \frac{y(1 + \frac{2}{n}) + \sqrt{1 + \frac{4}{n}(1 + \frac{1}{n})y^2}}{1 - y}, \tag{4.16}$$

$$r_+^n = \frac{M^2}{4xJ}\frac{y}{1 + \frac{1}{n}}\left[1 + \frac{2}{n} - \sqrt{1 + \frac{4}{n}\left(1 + \frac{1}{n}\right)y^2}\right]. \tag{4.17}$$

From these expressions, one can also see that physical solutions are restricted to the range $0 \le y \le 1$. Substituting these expressions into Eq. (4.14) then yields $S(y)$. Plotting the entropy, one finds that it vanishes[6] at $y = 0$ and 1 and that it has a single maximum in between. The value of $y_{\max}$ can be determined analytically to be

$$y_{\max}^2 = \frac{\sqrt{(1 + \frac{2}{n})(1 + \frac{1}{n} + \frac{1}{4n^2} + \frac{1}{2n^3})} - 1 + \frac{1}{2n} + \frac{1}{n^2}}{4(1 + \frac{1}{n})(1 + \frac{2}{n})}. \tag{4.18}$$

Now we would like to compare our results to those for the five-dimensional solution (4.1). For $n = 1$, Eq. (4.18) yields $y_{\max} \simeq 0.375$ for our loop of black string while Eq. (4.11) yields $y \simeq \sqrt{2}/3 \simeq 0.471$ for the large radius limit of the exact solution. Hence our model does not precisely reproduce the leading result for the large ring;

[6]This vanishing occurs because r_+^n vanishes at these points, as can be seen in Eq. (4.17).

however, the discrepancy is only of the order of 20%. Given the simplifying assumptions of our black string model, it seems to work surprisingly well.

We have found another interesting verification of our model as follows: In the limit of large n, Eq. (4.18) yields $y^2_{\max} \simeq 1/2n$ and, further, Eqs. (4.16) and (4.17) indicate that $\beta \simeq 1/\sqrt{2n}$ and $r^n_+ \propto 1/\sqrt{2n}$, respectively. Hence, in this limit (of a large space-time dimension), the string loop is very large and thin while its tangential velocity is small. Therefore it seems reasonable to treat the loop as a nonrelativistic mechanical string whose equilibrium configuration can be analyzed with Newton's law: $p v/R = T_{\rm tot}/R$ where the right-hand side is the centripetal acceleration of a small element of string with a linear momentum density p while the force on the left-hand side is determined by the total tension. Now applying a nonrelativistic limit to the stress tensor of the black string (3.5) yields

$$T_{tz} = \rho v, \qquad T_{zz} = -T + \rho v^2, \tag{4.19}$$

where we distinguish the mass density ρ and the tension T of the string. For the black string, Eq. (3.5) gives $T = \rho/n = \Omega_{n+1} r^n_+/16\pi G$ and so we note that we have $T \ll \rho$ for large n, as expected for a nonrelativistic string. Now setting $p = T_{tz}$ and $T_{\rm tot} = -T_{zz}$, the force law yields $v^2 = T/2\rho = 1/2n$ which precisely matches the model result quoted above.

Hence, it seems that we already have a fairly reliable model of the black string. Further this model is constructed for an arbitrary space-time dimension and so we conclude that black rings also exist in dimensions higher than five. In fact, for large dimensions, it seems that a large black ring will be spinning nonrelativistically.

Of course, our simple string model will only capture the leading behavior of Eq. (4.11) and not the gravitational or rigidity corrections. While we do not do so here, one could try improving our calculations to take these effects into account. In fact, one indication of the importance of these effects comes from the black ring solution itself. Note that it has been observed [30] that in the limit of large radius, the five-dimensional black rings are fairly relativistic in that $\sinh^2\beta \to 1$, in contrast to our results for large dimensions above. It is interesting that this boost corresponds precisely to where the tension (3.5) of the five-dimensional black string vanishes [30], i.e., $T_{zz} = 0$. Further, however, looking at (4.9) more carefully, we find

$$\sinh^2\beta = \frac{1+\nu^2}{1-\nu^2} \simeq 1 + 2\nu^2 \tag{4.20}$$

and the black ring actually seems to approach $\sinh^2\beta = 1$ from above as $\nu \to 0$, where the tension of the string would be negative. Of course, our model only results in a boost where the black string tension is positive and so can stabilize the spinning loop. However, the implication of Eq. (4.20) is that the stress tensor of the black string (3.5) must receive ''rigidity'' corrections, e.g., $1/R^2$ terms as in [31], when the string is drawn into a loop so that the tension remains positive in this limit. Similarly, the gravitational self-interaction may play a more important role here.

We can also use the black string model to extend our results for the Gregory-Laflamme instability of boosted black strings to black rings. In particular, the string loop will be subject to a Gregory-Laflamme instability when $k_{\max} R \gtrsim 1$. Using Eq. (3.18) and Table I, we have $k_{\max} = \cosh\beta \tilde{k}_{\max} \simeq 0.876 \cosh\beta/r_+$. Further evaluating these expressions with Eqs. (4.16), (4.17), and (4.18) with $n = 1$ gives an instability for

$$j^2 \gtrsim 0.239, \tag{4.21}$$

where j^2 is the reduced spin introduced in Eq. (4.7). There we also showed that for the five-dimensional black ring, the minimum value was $j^2_{\min} = 27/32 \simeq 0.844$ at $\nu = 1/2$. Hence, in accordance with the result at the end of the previous section, these calculations seem to indicate that all of the black ring solutions will be unstable. However, our model calculations need not be reliable for small values of j^2, i.e., for small black rings.

Before addressing the latter question, let us consider a slightly different approach to evaluating the threshold for the instability of the black ring. We reconsider our model of a loop of black string with three independent parameters. As above, we fix the mass and angular momentum which leaves one free parameter, which we take to be the radius of the loop. Now, rather than extremizing the entropy, here we require that the proper area of the horizons be the same. Again this gives three equations determining the model parameters, $R_{\rm model}$, r_+, β, now in terms of the two free parameters of the black ring, R and ν.

This system of equations fixes the rapidity to be

$$\sinh\beta = 1. \tag{4.22}$$

It is interesting that this corresponds to the boost for which the five-dimensional black string becomes tensionless, i.e., $T_{zz} = 0$, as is appropriate for the large-ring limit. Note here though that we have not explicitly taken such a limit. The remaining parameters are found to be

$$R_{\rm model} = \frac{(1+\nu)^2}{1+\nu^2} R, \tag{4.23}$$

$$r_+ = \frac{\sqrt{1-\nu^2}}{1+\nu^2} \nu R. \tag{4.24}$$

Note that $R_{\rm model}$ and R agree in the large-ring limit, $\nu \to 0$ but, in general, $R_{\rm model} > R$.

Returning to the Gregory-Laflame instability, the string loop will suffer from the instability when $k_{\max} R_{\rm model} \simeq 1$ with

$$k_{\max} = \tilde{k}_{\max} \cosh\beta = \frac{1.239}{\nu R} \frac{1+\nu^2}{\sqrt{1-\nu^2}} \tag{4.25}$$

where again we have used the five-dimensional result for

$\tilde{k}_{\rm max}$. Let us consider this threshold more carefully here. The validity of this model calculation (and that above) requires that the unstable modes are localized near the horizon on a scale much smaller than the size of the ring. This is, of course, because our calculations for the instability of the boosted string assumed an asymptotically flat metric and so we may only apply these results here if the perturbation is insensitive to the geometry at the antipodal points on the ring. Here we are considering the characteristic size of the modes in the direction orthogonal to the string and hence orthogonal to the boost direction. Therefore this profile is independent of the boost velocity and, for the threshold mode, we can again use the results from Sec. II. The radial falloff of this perturbation was determined by the scale $\tilde{\mu} = \sqrt{\tilde{\Omega}^2 + \tilde{k}_{\rm max}^2} = \tilde{k}_{\rm max}$ since $\tilde{\Omega}$ vanishes for the threshold mode. Given the boost factor, (4.22) is order one; the wavelength and the radial extent of the threshold mode are about the same size.[7] Hence, to be confident of our calculations for the black ring instability, the estimate above must be revised to $k_{\rm max} R_{\rm model} \gg 1$, which is equivalent to

$$\frac{\nu\sqrt{1-\nu^2}}{(1+\nu)^2} \ll 1.239. \tag{4.26}$$

Notice that the expression on the left-hand side has a maximum of 0.192 at $\nu = 1/2$ and hence we can be confident that this inequality will be satisfied, in general.

To summarize then, for any black ring on either branch in Fig. 6, one can find a corresponding black string model that has the same energy, spin and area. This version of the calculation again suggests that the black rings are unstable with a Gregory-Laflamme instability for any value of the parameters. However, we must note that this calculation is not always reliable. Recall that our underlying assumption was that the dominant black ring dynamics was simply determined by the rest energy and tension of the string. While this is indeed valid for the large black ring (small ν), Eq. (4.11) clearly shows that this assumption becomes invalid when ν grows. In particular, there is no reason that it should be trusted when $\nu \geq 1/2$ where the gravitational self-interaction will be important. For a conservative bound, we might require that ignoring the gravitational correction introduces less than a 10% error in the total energy, which means that we require $\nu \leq 0.05$. Of course, this bound is subject to the reader's taste in the admissible error and, in any event, it only represents a bound on one's confidence in the validity of our model. However, these calculations certainly do indicate that the black rings in Fig. 6 already experience a Gregory-Laflamme instability when the reduced spin j^2 is of order one.

[7]Note that we expect the threshold mode has the least radial extent of the unstable modes.

V. DISCUSSION

We considered the Gregory-Laflamme instability for boosted black strings. In the static frame, the results are largely unchanged compared to the instability of a static black string, although the boundary conditions required a complex frequency with a small imaginary component. However, the instability is strongly dependent on the boost velocity in the physical frame, as shown in Fig. 3(a) for $n = 1$. Since the threshold mode is by definition time independent, the mode found for the static black string is also a solution satisfying the appropriate boundary conditions in the static frame of the boosted string. As a result, for a fixed horizon size, there is a simple kinematical relation (3.18) between the threshold wave number of the static and boosted black strings. For the boosted black string, the threshold mode is a traveling wave moving in the z direction with precisely the same speed as the boosted string.

In the static case, Sorkin [16] showed that *stable* black strings and small black holes on a compact circle only coexist below a critical space-time dimension, of approximately 13. For the boosted case, in which there is internal momentum in the circle direction, we seem to find that this critical dimension is boost dependent and in fact vanishes for large boosts. This result is illustrated in Fig. 4 by the crossing of the curves for the minimal radius found from the Gregory-Laflamme analysis and from a comparison of the entropy of the black holes and strings.

Sorkin's result has interesting implications for the phase diagram for black objects in a compactified space-time [14,21]. For $5 \leq D \leq 13$, there is a regime where black holes and stable black strings coexist. These families of solutions are connected by a family of unstable and nonuniform black strings. For $D > 13$, the stable black strings and black holes do not coexist and the family of nonuniform black strings connecting these two phases is now expected to be stable.

Interest in the nonuniform black strings alluded to above began with the discussion of [34]. Such nonuniform solutions were first constructed perturbatively by Gubser in five dimensions [29] and this construction is straightforwardly extended to any number of space-time dimensions. Wiseman also used numerical techniques to find such strings in a fully nonlinear regime in six dimensions [25]. Here we observe that these nonuniform strings can be boosted to carry KK momentum in the internal direction. First, note that these solutions are static and periodic in, say, the $\tilde{z}$ direction with period $2\pi\tilde{R}$. Hence one can compactify these solutions by imposing the identification

$$(\tilde{t}, \tilde{z}) = (\tilde{t} + 2\pi\tilde{R}\tanh\beta, \tilde{z} + 2\pi\tilde{R}). \tag{5.1}$$

Now upon boosting as in Eq. (3.14), one arrives at a boosted frame where the identification is now $(t, z) = (t, z + 2\pi R)$ where $R = \tilde{R}/\cosh\beta$. Hence, in the physical (t, z) frame, one has a nonuniform string moving with

velocity $\tanh\beta$ along the z direction. Note, however, that we would not compare nonuniform and uniform black strings with the same boost factor. As in Sec. III A, any comparison would fix the total mass and KK momentum, as well as the circle radius, and since the ratio of the energy density and tension of the nonuniform and uniform strings is different, so would be the boost factors for each.

Now our observation on the boost dependence of the critical dimension would have interesting implications for the nonuniform strings. As in the static case, it would seem that for $D > 13$ these strings are stable for any value of the boost. On the other hand, for $5 \leq D \leq 13$, the nonuniform strings would apparently be unstable for low values of the boost; however, they become stable for large boosts. Note that in contrast to the uniform string which has a continuum of unstable modes, the static nonuniform string is expected to have a single unstable mode below the critical dimension reflecting the periodicity of the solution [14]. While imposing the ''boosted'' boundary condition (5.1) did little to modify the spectrum of unstable modes for the uniform black string, it seems to be enough to remove the unstable mode in the nonuniform case. It would be interesting then that these nonuniform boosted black strings may then form the end state for the decay of the uniform black strings with KK momentum.

We also applied our results for the instability of boosted strings to consider the analogous instability of the black rings of Emparan and Reall [6]. Both the naive discussion around Eq. (4.10) and the more detailed analysis in Sec. IV A seem to indicate that the entire branch of large-ring solutions is unstable. However, these are both expected to be reliable for small ν and so one must limit the application of our calculations. However, our results certainly indicate that Gregory-Laflamme instabilities will afflict the black rings already when the reduced spin j^2 is of order one. Hence it seems that this instability will enforce a Kerr-like bound on this particular family of solutions. This is then similar to the results of [15] where it was argued that the Gregory-Laflamme instability played a role in destabilizing ultraspinning black holes in $D \geq 6$, i.e., the only stable spinning black hole solutions in higher dimensions would have $J^{n+1} \lesssim GM^{n+2}$, i.e., $j^2 \lesssim 1$ for $D = 5$. There it was also argued that the five-dimensional spinning black holes may also become unstable near $j^2 = 1$ since there exist large black rings with the same spin and mass but a larger horizon area. Recently, it has also been argued that the small-ring branch is unstable using a thermodynamic treatment [35,36]. This result may have been anticipated since again there are always spinning black holes and large rings with the same mass and angular momentum but a larger horizon area.

Regarding the internal KK momentum as a charge, it is interesting to compare our instability results with those for black strings carrying a gauge charge [13,37], i.e., an electric three-form charge or a magnetic $(n + 1)$-form. Consistent with the gauge-charged string, the maximum value of the growth rate Ω of the unstable modes decreases (in the physical frame) as the KK momentum is increased, as illustrated in Fig. 3(a). However, one should actually think of the boosted strings as becoming more unstable as the KK momentum grows, since the physical threshold wave number $k_{\max}$ grows as the boost factor is increased, as described above. In contrast, increasing the gauge charge makes the black string more stable by decreasing the wave number of the threshold mode and it is expected to be absolutely stable in the extremal limit [37]. Note that the boosted string does not have an extremal limit as $v \to 1$, but rather the horizon becomes a null singularity in this limit.

We should also contrast our results with those in [17,38,39], which consider the Gregory-Laflamme instability for various black branes in string theory with D0-brane charge smeared over their world volume. In this case, the D0 charge is introduced by lifting the black brane from ten to 11 dimensions and boosting in the extra dimension. In contrast to the present case, there the boost direction and the directions along which the unstable modes form are orthogonal. Then, in accordance with the discussion here, the threshold for the boosted solution is unchanged from that for the original solution, i.e., with and without the D0 charge [38]. Similar boosts of nonuniform black strings have also been considered to generate new brane solutions in string theory [40].

Both t and z remain Killing coordinates for the gauge-charged strings and it is straightforward to consider boosting these solutions to form black strings carrying both KK momentum and gauge charge. In this case, the threshold for the Gregory-Laflamme instability would again satisfy the same kinematical relation (3.18) with that for the static string, if we fix the positions of the inner and outer horizons, $r_{\pm}$. Hence the extremal string ($r_+ = r_-$) will remain stable even after boosting. One should note that, just as boosting increases the energy density of the static string, it also increases the gauge-charge density.

The stability of the latter is then relevant for the large radius limit of the ''dipole-charged'' black rings [10]. The latter are five-dimensional black rings providing a local source of an electric three-form charge. This dipole charge is not a conserved charge and so these solutions introduce an infinite degeneracy of solutions with the same mass and angular momentum [10]. Given the above comments, we expect that introducing a dipole charge on the black rings will make them more stable. In particular, there should be a family of extremal rings which are exactly stable for any radius. If one adds further monopole charges, there also exist supersymmetric black rings [41,42] which must also be absolutely stable.

The stable dipole-charged rings then include stable solutions where J^2/GM^3 becomes arbitrarily large [10]. Hence, while there is a dynamical Kerr-like bound for

the vacuum solutions, as discussed above, no such bound holds in general. Therefore, if there is such a bound in higher dimensions, it must be a more refined version of the Kerr bound, perhaps defined in terms of angular momentum confined to a finite-size system. Certainly there is no problem producing configurations with an arbitrarily large (orbital) angular momentum by taking slowly moving bodies with very large separation, even in four dimensions, but, of course, we do not expect any such Kerr bound to apply to such systems.

While our discussion has focused on the Gregory-Laflamme instability affecting black rings, it is possible that these solutions may suffer from other instabilities as well. For example, rapidly rotating stars (as modeled by self-gravitating incompressible fluids) are subject to non-axisymmetric ''bar-mode'' instabilities when the ratio of the kinetic and gravitational potential energies is sufficiently large [43]. Given the discussion of Sec. IVA, large black rings are certainly in this regime and so one may suspect that they suffer from a similar instability. It might be that such instabilities restore the Kerr bound for black rings with dipole charges but they cannot play this role in general, as again the supersymmetric black rings must be absolutely stable.[8]

To consider bar-mode instabilities, one might extend the discussion of Sec. IVA to produce a model of the black ring which is not inherently axisymmetric. The analysis of Sec. III yields the energy density and tension of a boosted black string and so one might consider a model in which the black ring is described by a loop of string with the same mechanical properties—this is essentially our model for a uniform spinning loop. However, this information is insufficient to model general nonaxisymmetric loops. Basically, one still requires an equation of state for the string. For example, the mechanical string could be considered a relativistic string characterized by its fundamental tension plus some internal degrees of freedom. However, there are many possibilities for the latter, e.g., massive or massless excitations, which would lead to different equations of state but which could still match the same properties for a uniform boosted string. Hence progress in this direction requires a greater understanding of the dynamical properties of the black string.

One of the interesting observations of Sec. IVA is that, at least in the large-ring limit, the black ring configuration is essentially determined by the energy density and tension of the static black string. Hence this invalidates arguments restricting black rings to five dimensions based on the interplay of the gravitational potential and centripetal barrier, which have the same radial dependence in precisely five dimensions. Rather it shows that there should be black ring solutions in any number of dimensions greater than four and it confirms the original intuition presented in [7] that the existence of black rings did not depend on the dimension of the space-time (as long as $D > 4$). Of course, explicitly constructing these solutions remains a challenging open problem. Undoubtedly, these are simply one part of the rich multitude of solutions and physics which remains to be discovered in higher dimensions.

[8]One can consider nonaxisymmetric deformations of the supersymmetric black rings [42] but one finds that the resulting solutions do not have smooth event horizons [44].

ACKNOWLEDGMENTS

It is our pleasure to thank Toby Wiseman for his collaboration in the early stages of this project. We also wish to thank Óscar Dias, Roberto Emparan, Barak Kol, Don Marolf and David Mateos for discussions and comments. Research at the Perimeter Institute is supported in part by funds from NSERC of Canada and MEDT of Ontario. R. C. M. is further supported by an NSERC Discovery grant. R. C. M. would also like to thank the KITP for hospitality in the final stages of completing this paper. Research at the KITP was supported in part by the National Science Foundation under Grant No. PHY99-07949.

[1] T. Kaluza, Sitzungsber. Preuss. Akad. Wiss. Berlin (Math. Phys.) **1921**, 966 (1921).

[2] O. Klein, Z. Phys. **37**, 895 (1926); Surv. High Energy Phys. **5**, 241 (1986).

[3] See for example G. T. Horowitz, in Proceedings of String Theory and Quantum Gravity '92, Trieste 1992, hep-th/9210119; M. Cvetic, Nucl. Phys. B, Proc. Suppl. **56**, 1 (1997); J. P. S. Lemos, in Proceedings of the 17th Brazilian Meeting on Particles and Fields, Serra Negra, Brazil, 1996, hep-th/9701121; D. Youm, Phys. Rep. **316**, 1 (1999), and the references therein.

[4] See Proposition 9.3.2 in S. W. Hawking and G. F. R. Ellis, *The Large Scale Structure of Space-time* (Cambridge University Press, Cambridge, England, 1973).

[5] See for example W. L. Smith and R. B. Mann, Phys. Rev. D **56**, 4942 (1997); M. Banados, Phys. Rev. D **57**, 1068 (1998); D. R. Brill, J. Louko, and P. Peldan, Phys. Rev. D **56**, 3600 (1997); S. Holst and P. Peldan, Classical Quantum Gravity **14**, 3433 (1997), and the references therein.

[6] R. Emparan and H. S. Reall, Phys. Rev. Lett. **88**, 101101 (2002).

[7] R. C. Myers and M. J. Perry, Ann. Phys. (N.Y.) **172**, 304 (1986).
[8] W. Israel, Phys. Rev. **164**, 1776 (1967); Commun. Math. Phys. **8**, 245 (1968).
[9] See for example M. Heusler, Helv. Phys. Acta **69**, 501 (1996); *Black Hole Uniqueness Theorems* (Cambridge University Press, Cambridge, England, 1996), and the references therein.
[10] R. Emparan, J. High Energy Phys. 03 (2004) 064.
[11] C. V. Vishveshwara, Phys. Rev. D **1**, 2870 (1970); F. J. Zerilli, Phys. Rev. D **2**, 2141 (1970); W. H. Press and S. A. Teukolsky, Astrophys. J. **185**, 649 (1973); S. Chandrasekhar, *The Mathematical Theory of Black Holes* (Oxford University Press, New York, 1985).
[12] R. Gregory and R. Laflamme, Phys. Rev. Lett. **70**, 2837 (1993).
[13] R. Gregory and R. Laflamme, Nucl. Phys. **B428**, 399 (1994).
[14] B. Kol, Phys. Rep. **422**, 119 (2006).
[15] R. Emparan and R. C. Myers, J. High Energy Phys. 09 (2003) 025.
[16] E. Sorkin, Phys. Rev. Lett. **93**, 031601 (2004).
[17] O. Aharony, J. Marsano, S. Minwalla, and T. Wiseman, Classical Quantum Gravity **21**, 5169 (2004).
[18] H. S. Reall, Phys. Rev. D **64**, 044005 (2001).
[19] D. J. Gross, M. J. Perry, and L. G. Yaffe, Phys. Rev. D **25**, 330 (1982).
[20] R. C. Myers, Phys. Rev. D **60**, 046002 (1999).
[21] B. Kol, J. High Energy Phys. 10 (2005) 049.
[22] D. R. Terno, Phys. Rev. Lett. **93**, 051303 (2004).
[23] M. I. Park, Classical Quantum Gravity **22**, 2607 (2005); B. Kol and E. Sorkin, Classical Quantum Gravity **21**, 4793 (2004).
[24] H. Kudoh and U. Miyamoto, Classical Quantum Gravity **22**, 3853 (2005).
[25] T. Wiseman, Classical Quantum Gravity **20**, 1137 (2003).
[26] H. Kudoh and T. Wiseman, Phys. Rev. Lett. **94**, 161102 (2005).
[27] B. Kol, E. Sorkin, and T. Piran, Phys. Rev. D **69**, 064031 (2004); T. Harmark, Phys. Rev. D **69**, 104015 (2004); E. Sorkin, B. Kol, and T. Piran, Phys. Rev. D **69**, 064032 (2004); D. Gorbonos and B. Kol, J. High Energy Phys. 06 (2004) 053; Classical Quantum Gravity **22**, 3935 (2005).
[28] J. L. Hovdebo and R. C. Myers (to be published).
[29] S. S. Gubser, Classical Quantum Gravity **19**, 4825 (2002).
[30] H. Elvang and R. Emparan, J. High Energy Phys. 11 (2003) 035.
[31] A. M. Polyakov, Nucl. Phys. **B268**, 406 (1986); H. Kleinert, Phys. Lett. B **174**, 335 (1986).
[32] U. Lindstrom, Phys. Lett. B **218**, 315 (1989).
[33] R. H. Price and K. S. Thorne, Phys. Rev. D **33**, 915 (1986); *Black Holes: The Membrane Paradigm*, edited by K. S. Thorne, R. H. Price, and D. A. Macdonald (Yale University Press, New Haven, CT, 1986).
[34] G. T. Horowitz and K. Maeda, Phys. Rev. Lett. **87**, 131301 (2001).
[35] G. Arcioni and E. Lozano-Tellechea, Phys. Rev. D **72**, 104021 (2005); hep-th/0502121.
[36] M. Nozawa and K. I. Maeda, Phys. Rev. D **71**, 084028 (2005).
[37] R. Gregory and R. Laflamme, Phys. Rev. D **51**, R305 (1995).
[38] S. F. Ross and T. Wiseman, Classical Quantum Gravity **22**, 2933 (2005).
[39] S. S. Gubser, J. High Energy Phys. 02 (2005) 040; J. J. Friess and S. S. Gubser, J. High Energy Phys. 11 (2005) 040.
[40] T. Harmark and N. A. Obers, J. High Energy Phys. 09 (2004) 022.
[41] H. Elvang, R. Emparan, D. Mateos, and H. S. Reall, Phys. Rev. Lett. **93**, 211302 (2004); Phys. Rev. D **71**, 024033 (2005); J. P. Gauntlett and J. B. Gutowski, Phys. Rev. D **71**, 025013 (2005); **71**, 045002 (2005).
[42] I. Bena and N. P. Warner, hep-th/0408106.
[43] S. Chandrasekhar, *Ellipsoidal Figures of Equilibrium* (Yale University Press, New Haven, CT, 1969).
[44] G. T. Horowitz and H. S. Reall, Classical Quantum Gravity **22**, 1289 (2005).